Kinetic analysis of the activation of transducin by photoexcited rhodopsin

Influence of the lateral diffusion of transducin and competition of guanosine diphosphate and guanosine triphosphate for the nucleotide site

Franz Bruckert,* Marc Chabre,‡ and T. Minh Vuong‡§

*Departement de Biologie Moleculaire et Structurale, Laboratoire de Biophysique Moléculaire et Cellulaire, Commissariat a l'Energie Atomique, Centre d'Etudes Nucléaires de Grenoble, B.P. 85X-F38041 Grenoble Cédex, France; and ‡Centre National de la Recherche Scientifique, Institut de Pharmacologie Moléculaire et Cellulaire, Sophia Antipolis, F06560 Valbonne, France

ABSTRACT The activation of transducin (T) by photoexcited rhodopsin (R*) is kinetically dissected within the framework of Michaelis-Menten enzymology, taking transducin as substrate of the enzyme R*. The light scattering "release" signal (Vuong, T. M., M. Chabre, and L. Stryer. 1984. *Nature (Lond.)*. 311:659–661.) was used to monitor the kinetics of transducin activation at 20°C. In addition, the influence of nonuniform distributions of R* on these activation kinetics is also explored. Sinusoidal patterns of R* were created with interference fringes from two crossed laser beams. Two characteristic times were extracted from the Michaelis-Menten analysis: t_{form}, the diffusion-related time needed to form the enzyme-substrate R*-transducin is 0.25 ± 0.1 ms, and t_{cat}, the time taken by R* to perform the chemistry of catalysis on transducin is 1.2 ± 0.2 ms, in the absence of added guanosine diphosphate (GDP) and at saturating levels of guanosine triphosphate (GTP). With t_{form} being but 20% of the total activation time $t_{form} + t_{cat}$, transducin activation by R* is not limited by lateral diffusion. This is further borne out by the observation that uniform and sinusoidal patterns of R* elicited release signals of indistinguishable kinetics. When [GDP] = [GTP] = 500 μM, t_{cat} is lengthened twofold. As the in vivo GDP and GTP levels are comparable, the exchange of nucleotides may well be the rate-limiting process.

INTRODUCTION

In the retinal rod outer segment (ROS), fast activation of the heterotrimeric G-protein transducin (T) by photoexcited rhodopsin (R*) and guanosine triphosphate (GTP) accounts for two important features of the light response: amplification and speed (Stryer, 1986). In situ, each R* takes a few milliseconds to activate one transducin (Vuong et al., 1984; Bruckert et al., 1988). Thus, within the duration of the physiological response to a light flash (Baylor et al., 1984), one R* may activate hundreds of transducin molecules. Transducin is a peripheral membrane protein consisting of three subunits: α, β, and γ. When holotransducin is by itself, its α-subunit always binds a nucleotide [either guanosine diphosphate (GDP) or GTP] and does not release it spontaneously. The nucleotide can be exchanged only when transducin interacts with R*.

Kinetically speaking, transducin activation by R* and GTP encompasses at least five steps (Fig. 1 *A*). Step 1 is the formation of a loose enzyme-substrate complex between R* and Tβγ-TαGDP (T-GDP), with both R* and transducin still retaining the conformations they had before the event. The forces that hold the two molecules together are still weak, some nonspecific electrostatic interaction, for example, that does not perturb the conformations. The forward rate constant k_{+enc} is due in large part to the diffusion of R* and T-GDP; that is, the time needed to establish the interaction between the two molecules is much less than the time they take to approach each other via lateral diffusion. The reverse rate constant k_{-int} is the inverse of the lifetime of this virtual bound state. There is a sort of dissymmetry between the forward and reverse processes: the former is largely a process of lateral diffusion, whereas the latter relates more to the contact interaction between R* and T-GDP. This is reflected in the notation adopted for the respective rate constants. Step 2 is a conformational change undergone by transducin and resulting in the opening of the nucleotide site on its α-subunit. Transducin is now modified and is denoted T‡ instead of T. Step 3 is the release of GDP from Tα, giving rise to a very tight R*-$T^{‡}_{empty}$ complex (Bornancin et al., 1989). Step 4 is the entry of GTP into this open, empty nucleotide site. Step 5 includes the closure of the site and the dissociation event where the three species R*, TαGTP, and Tβγ separate from each other. The active TαGTP leaves the disc surface and gets solubilized into the surrounding medium. R* has thus acted as a catalyst, and the whole process can be described with a classical Michaelis-Menten scheme (Fig. 1 *B*). The formation of the enzyme-substrate R*-T‡-GDP corresponds to step 1 and 2, whereas catalysis encompasses steps 3–5. Invoking the transient state R*.T-GDP is but a formal way to describe the early binding of the substrate T-GDP to the enzyme R*. Because we cannot observe this transient state, the simpler scheme of Fig. 1 *B* will suffice for the interpretation of many of our results; when a more detailed treatment is needed, we shall refer only to steps 3–5 of Fig. 1 *A*. In Fig. 1 *B*, the second-order rate constant for the formation of R*-T‡-GDP, k_{form}, is proportional to the encounter rate constant k_{+enc}, the proportionality constant α being the efficiency of collision. α could be expressed in terms of k_{-int}, k_{+cnf}, and k_{-cnf}, but this would be pointless because their numerical values are experimentally inaccessible. The same remarks pertain to k_{off}, the rate constant for the dissociation of R*-T‡-GDP.

The chemistry of these reactions exhibits two special features. (*a*) Transducin activation takes place in the two-dimensional environment of the disc membrane,

Address correspondence to T. Minh Vuong.

0006-3495/92/09/616/14 $2.00

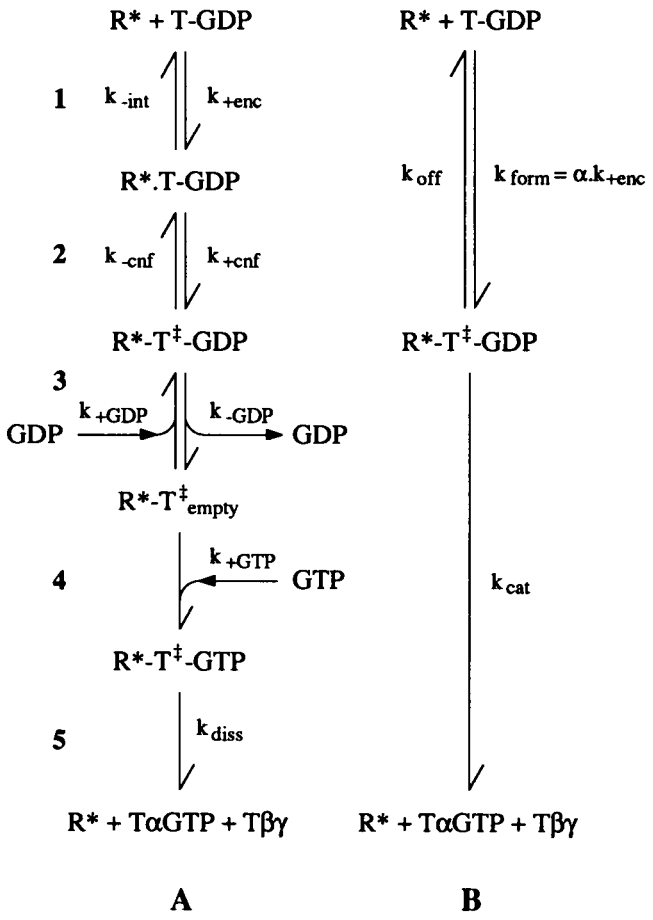

FIGURE 1 Reaction schemes for the activation of transducin by R*. (*A*) The detailed scheme consists of five steps as described in the text. (*B*) Compressed scheme to recast the activation process in a Michaelis-Menten framework. The formation of the enzyme-substrate complex, R*-T‡-GDP, comprises steps 1 and 2 of the detailed scheme. The chemistry of catalysis is made up of steps 3, 4, and 5.

the enzyme R* and its substrate T-GDP coming together via lateral diffusion. Therefore, all concentrations must be expressed in molecules per unit area, or more conveniently, relative to the concentration of the membrane-bound rhodopsin. (*b*) The association of T-GDP with the disc is not infinitely tight. In vivo, the transducin concentration is very high inside the intact ROS, and the great majority of the transducin pool is bound to the disc surface. In vitro, if the ROS is made leaky and the membrane concentration is low, the equilibrium $(T\text{-}GDP)_{mb} \leftrightarrow (T\text{-}GDP)_{sol}$ is shifted to the right (Liebmann and Sitaramayya, 1984); a portion of the inactive transducin gets solubilized even before any light flash.

The overall speed of the activation of transducin by R* was already measured using light scattering from oriented frog ROS fragments (Vuong et al., 1984). The activation of each T-GDP by an R* was estimated to take about 1 ms, assuming the whole pool of holotransducin to be membrane bound. Given the necessarily low concentrations of ROS membranes used in those early experiments (~0.1 mg rhodopsin/ml), one must expect a substantial portion of holotransducin to be already solubilized in the dark. Bruckert et al. (1988) were able to control and measure the amount of T-GDP remaining on the disc in these conditions of low membrane concentrations. With this new knowledge, the activation time of transducin by R* may have to be revised upward. The question now arises as to how this transducin activation time should be divided among the steps described above (Fig. 1 *A*). It has often been assumed that the rate-limiting step in this activation scheme is the diffusion-mediated encounter between R* and T-GDP, i.e., step 1 (Stryer, 1986; Liebman et al., 1987). This hypothesis calls for a measurement of the lateral diffusion coefficient of T-GDP on the disc surface. As the diffusion coefficient is already known for R* (Poo and Cone, 1974), one could then estimate the time it takes for R* and T-GDP to come together and compare it with the overall activation time of a few milliseconds. However, such a direct measurement of the lateral diffusion coefficient of transducin is at the present not feasible.

In the present work we attempt to approach the problem indirectly in two ways. First, the effects of varying the T-GDP surface concentration on the transducin activation kinetics is studied. The technique of near infrared light scattering on oriented ROS (Vuong et al., 1984; Bruckert et al., 1988) is used to measure the concentration of membrane-bound transducin, through the amplitudes of the "loss" and "binding" signals, and to follow its activation after a light flash, through the kinetics of the "release" signal. Using a Michaelis-Menten treatment, we arrive at a lower limit for the lateral diffusion coefficient of transducin. The effects of relative nucleotide concentrations (i.e., [GTP]/[GDP]) are also explored to search for a possible contribution of the exchange steps to the overall catalysis time. Second, the influence of an initially nonuniform spatial distribution of R* in the disc membrane on the activation kinetics is investigated. The light-scattering apparatus was modified so that the rhodopsin in the oriented ROS could be photoexcited nonuniformely with interference fringes from two crossed laser beams; stripes of R* were created on the disc surface (Fig. 2). Within the bright fringes, the local concentration of T-GDP would quickly decrease as it gets activated by R*, but within the dark fringes, where little R* is present, the T-GDP concentration should be relatively unchanged. The creation of R* fringes thus results in fringes of T-GDP of opposite phase. Under certain conditions, activation of the total pool of transducin would be delayed as there is now the additional time needed for T-GDP and R* to diffuse across half a fringe spacing. This delay ought to be reflected in the kinetics of the light-scattering signal that monitors transducin activation.

MATERIALS AND METHODS

All light-scattering experiments were performed under dim red light, using ROS extracted from freshly dissected frog retinas and free of

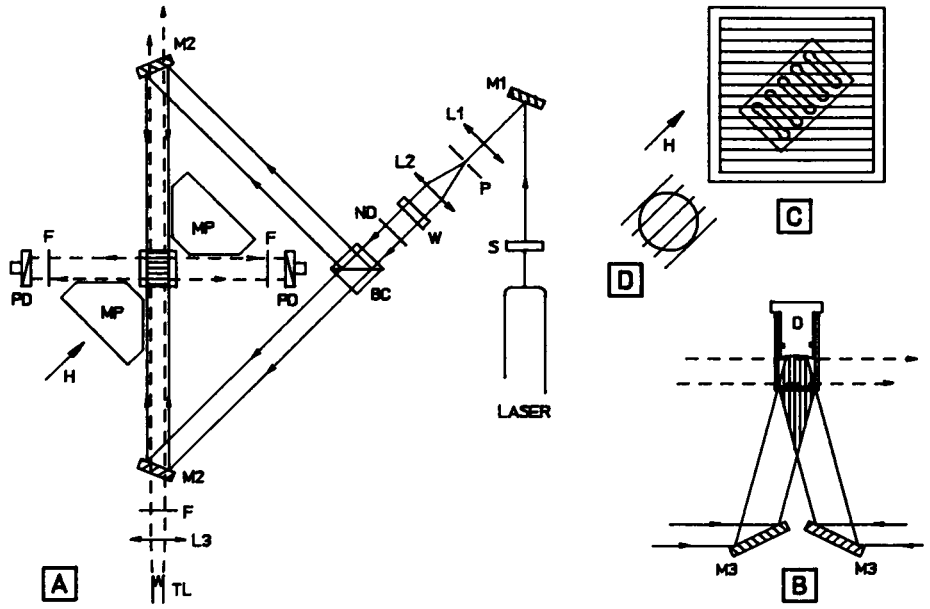

FIGURE 2 Schematic diagram of the optical setup. (*A*) Top view. The visible laser light is shown in solid lines, whereas the dashed lines represent the infrared beam. *BC*, beamsplitter cube; *F*, 850-nm lower cutoff glass filter (model 51360; Oriel Corp. of America, Stamford, CT); *H*, orienting magnetic field; *L1*, *L2*, lenses; *M1*, *M2*, mirrors; *P*, 30-μm pin hole; *MP*, magnet pole pieces; *ND*, 0.3 OD neutral density filter; *PD*, PIN photodiodes (UDT sensors, United Detector Technology, Hawthorne, CA); *S*, electromechanical shutter (Vincent Associates, Rochester, NY); *TL*, quartz-halogen tungsten lamp; *W*, quarter-wave plate (Spindler-Hoyer, Milford, MA). (*B*) Side view of the cuvette. The two mirrors *M3* send the laser beams into the cuvette where they form an interference zone that is probed by the infrared beam (dashed lines). A black delrin plug (*D*) prevents formation of a meniscus. (*C*) Top view of an oriented rod and of the interference fringes in the cuvette. (*D*) Front view of an oriented rod in the interference fringe region; the disc surface is crossed by five fringes.

pigment epithelium. Retinas to which some black epithelium remained attached were used as source of extracted transducin.

Three buffers were employed. (*a*) For retina dissection, an isotonic solution containing (mM): NaCl 102, KCl 2.7, $MgCl_2$ 2.1, $CaCl_2$ 1.9, $NaHCO_2$ 2.0, NaH_2PO_4 0.36, pH 7.4. (*b*) For the ROS suspension a solution of the same composition except that the phosphate-carbonate was replaced by 10 mM tris(hydroxymethyl)-aminomethane-acetate, pH 7.4. (*c*) For transducin extraction an hypotonic solution containing (mM): $MgCl_2$ 0.1, *N*-2-hydroxyethylpiperazine-*N'*-2-ethane sulfonic acid 2.5, pH 7.4. All buffers were degassed and supplemented with phenylmethylsulfonyl fluoride (0.1 mM) and dithiothreitol (1 mM) ~10 min before use. GDP and GTP stock solutions (5 or 10 mM) were prepared in isotonic buffer (pH 7.4).

Preparation of ROS

Frog ROS were prepared according to the usual procedure (Chabre, 1975): freshly dissected retinas are shaken in isotonic buffer and filtered through gauze (~2 retinas/ml). ROS were separated from small membrane debris by gentle (280 *g*, 2 min) centrifugation and resuspended in isotonic buffer at a concentration of ~5 retinas/ml. This stock suspension was stored on ice and used within 2 h.

Permeabilization of ROS

Two techniques were used: mechanical fragmentation and, for the interference fringe experiments, electroporation. For mechanical fragmentation, the ROS suspension (0.5 mg rhodopsin/ml) was passed three times through a constricted hypodermic needle (21 gauge, 0.8 mm ID). The mechanical shearing yields 10-μm-long fragments leaky to nucleotides and transducin. For electroporation, brief (10 ms) electric pulses (1 KV/cm) can irreversibly permeabilize the plasma membrane of cells 10 μm in size (Zimmermann, 1982). We installed between the pole pieces of an electromagnet (0.8 T) a 300-ml cuvette equipped with two parallel flat electrodes 5 mm apart. The magnetic field ensures that all ROS have their axes oriented at 90° to the electric field. The rest of the device consists of a high voltage power supply (2 kV), a capacitor, and a mercury-wetted switch. Routinely, we apply three exponential pulses (4 kV/cm, τ = 40 ms) 20 s apart to the ROS suspension (0.5 mg rhodopsin/ml); >95% of the ROS are thus permeabilized. Electroporated ROS were stocked at 0°C and used within 2 h of their preparation.

Extraction of transducin

The extraction was done according to Kühn (1981). ROS from a concentrated (10 retinas/ml) suspension were mechanically fragmented and sedimented at 4×10^5 *g* for 3 min in a centrifuge (model TL100, Beckman Instruments, Inc., Fullerton, CA). The supernatant was discarded, the pellet was illuminated, and resuspended in hypotonic buffer to extract the cGMP-phosphodiesterase. After sedimentation, the pellet was again resuspended in the same volume of hypotonic buffer supplemented with 60 μM GTP. A last centrifugation yielded an extract in which transducin constitutes >90% of total proteins as estimated from densitometry of Coomassie-blue stained sodium dodecyl sulfate-polyacrylamide gel electrophoresis (SDS-PAGE).

Supplementing permeabilized ROS with transducin extract

Permeabilized frog ROS suspensions (0.5 mg rhodopsin/ml) were incubated for 3 min with crude transducin extract in isotonic buffer at room temperature to obtain the final concentration needed for the experiment. The preparation was immediately used. Binding of transducin was checked by SDS-PAGE on sedimented ROS pellet aliquots as described previously (Bruckert et al., 1988). GTP and GDP (when needed) were added to the ROS suspension just before the cuvette was

put into the light scattering set up. The first flash was triggered about 4 min later, because this is the time it took the ROS sample to stabilize in the magnetic field. The time interval between measurements on successive samples was 6–9 min. From the moment the ROS were detached from the retinas, a complete set of experiments took ~2 h. The transducin extracts were used within 4–5 h of extraction.

Infrared light scattering setup

The light scattering geometry used here was already described previously (Vuong et al., 1984; Bruckert et al., 1988). Briefly, the ROS in a 1-cm-path length quartz cuvette (volume 1.3 ml) were magnetically oriented at 45° to the incident infrared beam ($\lambda > 850$ nm), in the horizontal plane, and could be flash illuminated from below. Scattered light at right angles to the left and right of the probing infrared beam was detected with PIN photodiodes (model PIN-10DP, UDT sensors) operating in the photovoltaic mode. Their output was digitized simultaneously at two different rates giving fast and slow recordings (of 512 points each) that were resistance-capacitance filtered (low-pass) at 2.5 and 50 ms, respectively. Distorsion due to the 2.5-ms filter is negligible because the release signal whose linear slope is used in this study has a time-to-peak of ~200 ms at $R^*/R = 10^{-3}$. This dual time-base recording conveniently resolves the various components of the dissociation and the binding signals. This experimental arrangement was the same for experiments using only uniform illumination as well as for those where rhodopsin was photoexcited with interference fringes. In the first case, a photographic flash unit fitted with a 500-nm interference filter and a series of neutral density filters uniformely illuminated the sample via a plexiglas light guide mounted below the cuvette.

Setup for illumination with interference fringe flashes

To obtain sinusoidal distributions of R* on the disc membranes, the visible light flash comes from an Argon ion laser (model 2020-03, 514-nm line Spectra-Physics Inc., Mountain View, CA). The laser beam is split in half and recombined inside the cuvette to produce interference fringes. For the control, only one of the two beams is used to produce a uniform distribution of R*. The optical setup is shown in Fig. 2. After spatial filtering and expansion ($1/e$ diameter = 25 mm), the Gaussian laser beam is split into two beams of equal intensity that travel toward the cuvette along symetrical paths. The two beams crossed at the center of the cuvette with part of the interference zone being inside it. The 30° angle between the crossed beams resulted in a fringe spacing of 0.7 μm. But as the long axes of the ROS are oriented 45° to the fringes, the spatial period of the R* stripe pattern on the disc surface is ~1 μm. The original vertical polarization of the laser beam is rotated 90° with a quarter waveplate. In this way, maximum fringe contrast is obtained since when the two beams interfere, their electric vectors are both horizontal and thus colinear. Fringe illumination is obtained with both split beams and a 0.3 OD neutral density filter on the main beam. Uniform illumination is obtained using only one of the split beams, blocking the other one but removing the 0.3 OD neutral density filter on the main beam to retain the same intensity. Flashes of ~4 ms in duration are produced with an electromechanical shutter (Vincent Associates, Rochester, NY) placed on the main beam.

The interference zone inside the cuvette took up ~70% of the sample volume (Fig. 4 *B*). To collect only the light scattered by the ROS in this volume, appropriate masks are installed so as to block scattered light coming from zones devoid of interference fringes. Since convection of the ROS in the cuvette is negligible on the time course of the fast dissociation signal, the scattered infrared light can be considered as coming only from ROS inside the interference zone. A specially shaped plug made of black delrin (Fig. 2 *B*) is used to cap the cuvette and prevent formation of a meniscus from which reflection of the laser beams would degrade the fringe pattern. With the delrin plug and the masks installed, the sample is 6 mm wide and 8 mm high.

At the usual ROS concentration of ~2.5 μM rhodopsin, the laser interference fringes are entirely scrambled after having traversed only 1 mm of the suspension. To surmount this difficulty, the following measures are taken. First, instead of small ROS fragments obtained via mechanical shearing, electroporated whole ROS are used as they diffuse less at the same rhodopsin concentration. Second, the ROS concentration is lowered until the interference fringes are intact after having traversed the 8 mm of ROS suspension. This critical concentration is determined by a visually inspecting the interference pattern formed by the two split beams as they emerge from the ROS suspension. A ROS sample of the same height as the actual one (8 mm) is placed in a special cuvette with a transparent bottom. The sample is covered with a microscope slide in order not to have a meniscus. The two emergent beams are collected by the objective of a microscope through which the resulting fringe pattern is observed. At a membrane concentration of 0.38 μM rhodopsin, the emerging beams, after having traversed the 8 mm of ROS suspension, still formed clean, unscrambled fringes.

Such dilute suspensions of ROS, however, pose two new technical challenges. First, at 0.38 μM rhodopsin, a major portion of the transducin pool gets solubilized even before the light flash; complementation with exogenous transducin extracted from other retinas is thus absolutely necessary. Second, the large unfragmented ROS sediment very quickly, leading to a loss of scattering signal. This can be avoided by suspending the ROS in buffer prepared with heavy water.

Steady-state analysis of transducin activation

Applying the classic Michaelis-Menten formalism to R* as the enzyme, T-GDP as its substrate and TαGTP and Tβγ as the products, we get the scheme of Fig. 1 *B*.

$$R^* + \text{T-GDP} \underset{k_{off}}{\overset{k_{form}=\alpha k_{+enc}}{\rightleftharpoons}} R^*\text{-T}^{\ddagger}\text{-GDP} \xrightarrow{k_{cat}} R^* + \text{T}\alpha\text{GTP} + \text{T}\beta\gamma.$$

As usual, the velocity V for this reaction, i.e., the rate of formation of TαGTP at steady state, is given by the Michaelis-Menten equation (Briggs-Haldane extension):

$$V = \left(\frac{d\{\text{T}\alpha\text{GTP}\}}{dt}\right)_s = \frac{k_{cat}\{R^*\}_s\{\text{T-GDP}\}_s}{\{\text{T-GDP}\}_s + K_M} \cong \frac{k_{cat}\{R^*\}_0\{\text{T-GDP}\}_0}{\{\text{T-GDP}\}_0 + K_M} \quad (1)$$

where K_M is the Michaelis constant. Steady-state and initial concentrations are denoted by the s and 0 subscripts, respectively. Braces denote surface concentrations. As explained below, the steady-state concentrations $\{R^*\}_s$ and $\{\text{T-GDP}\}_s$ can be approximated by their initial values. Furthermore:

$$k_{form} = \frac{k_{cat} + k_{off}}{K_M}. \quad (2)$$

As usual, k_{cat}/K_M tells us something about the diffusional aspects of the process as it is a lower bound for k_{form}. Indeed, the rate constant for the formation of the R*-T*-GDP complex, k_{form}, depends on the diffusion coefficients D_R and D_T of R* and T-GDP, respectively, through the encounter rate constant k_{+enc}. k_{off} and hence k_{form} are not directly measurable, but from Eq. 2, a lower bound for k_{form}, and therefore for D_T, is simply k_{cat}/K_M. From Eq. 1, k_{cat} and K_M can be deduced from the dependence of the velocity V on the substrate concentration $\{\text{T-GDP}\}_0$. V is measured as the maximum slope of the release signal. The enzyme concentration $\{R^*\}_0$ is easily obtained as it is simply related to the photolysis level. The measurement of $\{\text{T-GDP}\}_0$, however, poses a major technical challenge. As said above, the amplitudes of the loss and

binding signals are used in meeting this challenge. The technical details of this procedure are elaborated further on.

Another way to see how the formation of R*-T‡-GDP, and hence indirectly the lateral diffusion of transducin, enters into the overall kinetics of activation is to consider, at some $\{R^*\}_0$, the time taken by one R* to activate one transducin. From Eq. 1 this activation time t_{act} is:

$$t_{act} = \frac{1}{k_{cat}} \frac{\{\text{T-GDP}\}_0 + K_M}{\{\text{T-GDP}\}_0} = \frac{1}{k_{cat}} + \frac{K_M}{k_{cat}\{\text{T-GDP}\}_0} = t_{cat} + t_{form} \quad (3)$$

t_{act} is thus the sum of the catalysis time, $t_{cat} = 1/k_{cat}$, and the time $t_{form} = K_M/k_{cat}\{\text{T-GDP}\}_0$ needed to form the R*-T*-GDP complex. Evidently, t_{form} is due in part to the lateral diffusion of transducin and R*. Knowing K_M and k_{cat}, one can estimate how much this process of lateral diffusion contributes to the overall activation kinetics at a given level of $\{\text{T-GDP}\}_0$.

As for the catalysis time t_{cat} itself, how might we kinetically dissect it? The open nucleotide site of $R^*\text{-}T^{\ddagger}_{empty}$ is equally accessible to both GDP and GTP. In the extreme case of a very high [GDP]/[GTP] ratio, this site is rarely filled with a GTP, and the forward reaction is therefore drastically slowed down. With a more reasonable [GDP]/[GTP] ratio, such as one found in the rod cell, how much does competition by GDP for the nucleotide site contribute to the millisecond time of activation? Consider the three steps of Fig. 1 *A* through which T-GDP is catalytically transformed into TαGTP and Tβγ. The chemistry is assumed to proceed forward irreversibly once GTP has entered into the nucleotide site, hence a k_{-GTP} does not appear in the scheme. The time t_{cat} can be written as a sum of three subtimes (Fersht, 1985), which are the transit times of these three steps:

$$t_{cat} = \frac{1}{k_{cat}} = t_{GDP} + t_{GTP} + t_{diss}$$

These three transit times can be expressed in terms of the various rate constants of Fig. 1 *A*:

$$t_{GDP} = \frac{1}{k_{-GDP}}$$

$$t_{GTP} = \frac{1}{k_{+GTP}[\text{GTP}]}\left(1 + \frac{[\text{GDP}]}{K_{GDP}}\right)$$

where

$$K_{GDP} = \frac{k_{-GDP}}{k_{+GDP}}$$

$$t_{diss} = \frac{1}{k_{diss}}$$

t_{GDP} is the time taken by GDP to leave the open nucleotide site, t_{GTP}, the time taken by GTP to enter into the now empty site, and t_{diss} is the time needed for dissociation to occur. The notion of a saturating GTP level is clearly borne out by the expression for t_{GTP}. As [GTP] increases, the GTP entry time t_{GTP} gets smaller compared with the other transit times that make up t_{cat} until t_{GTP} can simply be dropped. The GTP entry time t_{GTP} consists of the "intrinsic" time $1/(k_{+GTP}[\text{GTP}])$, multiplied by a "modifying" factor that increases linearly with [GDP]. This then is just another way of saying that GDP competes with GTP for the same nucleotide site. When [GDP] is large compared with its affinity K_{GDP}, the GTP entry time t_{GTP} is lengthened by an amount Δt_{GTP} given by:

$$\Delta t_{GTP} = \frac{1}{k_{+GTP}K_{GDP}} \frac{[\text{GDP}]}{[\text{GTP}]} = t_{GDP} \frac{k_{+GDP}[\text{GDP}]}{k_{+GTP}[\text{GTP}]}.$$

Physically, this means that once at the $R^*\text{-}T^{\ddagger}_{empty}$ stage, the reaction can proceed forward with a rate $k_{+GTP}[\text{GTP}]$ or backward with a rate $k_{+GDP}[\text{GDP}]$. If it goes backward, an additional $R^*\text{-}T^{\ddagger}\text{-GDP} \rightarrow R^*\text{-}T^{\ddagger}_{empty}$ transition will be required, taking an extra characteristic time t_{GDP}. This slow-down due to GDP should not affect the final amount of transducin activated. It takes longer to reach the product stage with GDP present because some of the time the nucleotide loading is "unsuccessful," thus requiring another try. But eventually the reaction does proceed forward to give the expected final products TαGTP and Tβγ.

Another way to look at this GDP effect is to rewrite t_{cat} as follows:

$$t_{cat} = t_{min} + \frac{1}{k_{+GTP}K_{GDP}} \frac{[\text{GDP}]}{[\text{GTP}]} \quad (4)$$

where

$$t_{min} = t_{GDP} + \frac{1}{k_{+GTP}[\text{GTP}]} + t_{diss}.$$

The minimum catalysis time, t_{min}, is obtained in the absence of GDP; also, t_{min} reduces to $t_{GDP} + t_{diss}$ if the GTP level is saturating.

The second term of Eq. 4 represents the "slow-down" due to competition by GDP; given a certain [GDP]/[GTP] ratio, what is the contribution of this "slow-down" to the overall catalysis time t_{cat}? The significant parameters are the rate of GTP entry, k_{+GTP}, and the affinity K_{GDP} of GDP for the open nucleotide site. Bennett and Dupont (1985) measured the binding of [^{3}H]GDP to illuminated ROS membranes in which there was a 10-fold excess of R*. Under these conditions, transducin is essentially in equilibrium between $R^*\text{-}T^{\ddagger}\text{-GDP}$ and $R^*\text{-}T^{\ddagger}_{empty}$, and the GDP affinity for the $R^*\text{-}T^{\ddagger}$ complex was $K_{GDP} = 20 \pm 10\ \mu M$. As for k_{+GTP}, using for the expression of $k_{cat} = 1/t_{cat}$, the Michaelis-Menten relation (1) can be rewritten as:

$$\left(\frac{d\{\text{T}\alpha\text{GTP}\}}{dt}\right)_s^{-1} = \frac{\{\text{T-GDP}\}_0 + K_m}{\{\text{R}^*\}_0\{\text{T-GDP}\}_0}\left(t_{min} + \frac{1}{k_{+GTP}K_{GDP}}\frac{[\text{GDP}]}{[\text{GTP}]}\right). \quad (4')$$

Thus, k_{+GTP} can be estimated from the slope of the linear plot of the inverse velocity as a function of [GDP]/[GTP].

In the above equations, [GDP] and [GTP] are both volume concentrations, whereas, as said before, $\{R^*\}_0$ and $\{\text{T-GDP}\}_0$ are surface concentrations. Similarly, k_{+GDP} and k_{+GTP} also refers to the bulk volume as they are in units of $M^{-1}\ sec^{-1}$. This does not raise any problems of dimensionality. Indeed the nucleotide concentrations and their bimolecular rate constants are always bundled together as first-order rate constants $k_{+GDP}[\text{GDP}]$ and $k_{+GTP}[\text{GTP}]$ that make no reference to surface or volume.

Near infrared light-scattering signals on oriented ROS

Illuminating with a visible light flash a dilute suspension of ROS in a near infrared light beam elicits two types of transient changes in the infrared scattered intensity: the "dissociation" signal obtained in the presence of GTP and the "binding" signal in its absence (Kühn et al., 1981; Bruckert et al., 1988). Magnetically orienting the ROS at 45° to the incident infrared beam and collecting the scattered light at 90° on the left and right sides (Vuong et al., 1984; Chabre, 1985) helps resolve the dissociation signal into two components: a fast (0.1 s), scattering increase observed only on the left side and a slow (1 s), isotropic scattering decrease observed equally in both directions. Vuong et al. (1984)

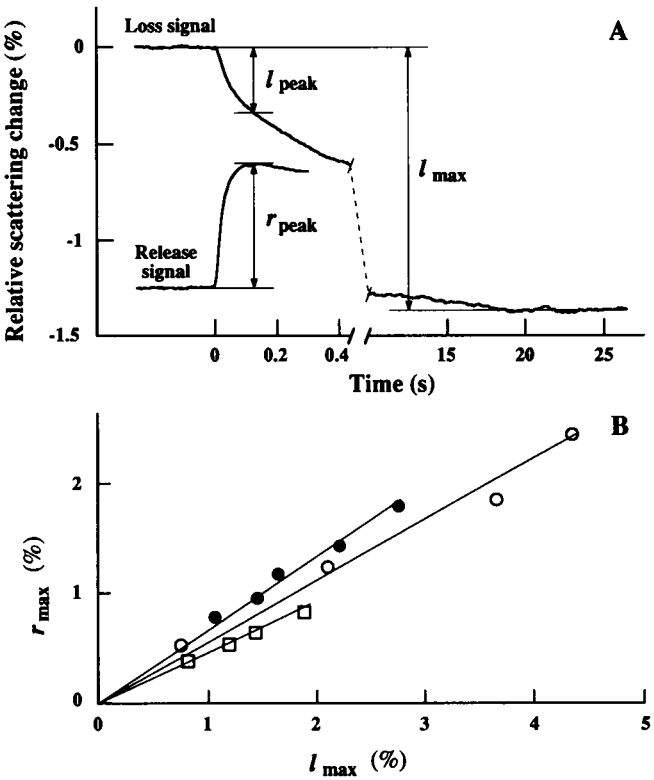

FIGURE 3 Calibration procedure to find C_{loss} and $C_{release}$. (*A*) For the loss signal, the baseline is taken between −15 and 0 s, and the saturated loss amplitude l_{max} is measured between 15 and 25 s. For the release signal, the baseline is taken between −0.2 and 0 s. The peak amplitude r_{peak} is measured between 0.1 and 0.2 s. l_{peak} is the amplitude of the loss signal when the release signal reaches its peak, r_{peak}. The corrected value r_{max} is computed from these determinations of l_{max}, l_{peak}, and r_{peak} (see text). (*B*) The saturated amplitude r_{max} of the release signal is plotted as a function of the saturated amplitude l_{max} of the loss signal; the slope of the fitted line is $C_{loss}/C_{release}$ (see text). $\{R^*\}_0/\{R\} = 4 \times 10^{-3}$; [GTP] = 1.5 mM (●), 0.7 mM (○), and 0.38 mM (□). For all three series, mechanical fragmentation of the ROS was performed with the same constricted hypodermic needle. The values of $C_{release}$ obtained varied between 1.46 and 2.01.

showed that the fast, anisotropic component is due to the release of TαGTP from the disk surface into the interdiscal space, whereas the slow, isotropic one corresponds to the subsequent loss of TαGTP from the leaky ROS fragments into the bulk solution. These two components are named "release" and "loss" signals, respectively (Fig. 3). The rising phase of the release signal thus closely reflects the kinetics of TαGTP formation. This release signal is extracted by subtracting the right side data from the left side data. The binding signal includes a fast (20 ms), partially anisotropic component and a slow (20 s) isotropic component (Bruckert et al., 1988). The fast component results from the interaction between R* and the transducin present on the disk membrane before the flash, $(T\text{-}GDP)_{mb}$. On illumination, this $(T\text{-}GDP)_{mb}$ binds tightly to R* and becomes nonexchangeable with the transducin in solution, $(T\text{-}GDP)_{sol}$. The $(T\text{-}GDP)_{mb} \leftrightarrow (T\text{-}GDP)_{sol}$ equilibrium is thus shifted to the left. The slow isotropic component monitors the rebinding of $(T\text{-}GDP)_{sol}$ to the disks and eventually to the R* in excess of the initial $(T\text{-}GDP)_{mb}$ pool (Schleicher and Hofmann, 1987). The exchange of T-GDP between membrane and solution is slow and can be ignored when considering the dissociation signal. The molecular origins of the loss signal and of the fast component of the binding signal suggest that they can both be used to assay for the membrane-associated transducin, $(T\text{-}GDP)_{mb}$. The term binding signal shall henceforth refer only to the fast binding component since the slow component is not used in the present work.

Concentration of membrane-bound transducin is evaluated from the amplitudes of the light-scattering binding and loss signals

The amplitudes of the binding and loss signals can both be used to assay for the amount of T-GDP residing on the disc surface of ROS supplemented or not with extracted transducin (Bruckert et al., 1988). Arising from the one-to-one R*-transducin interaction, the fast binding signal reaches its saturated amplitude when the $\{R^*\}$ created by the flash equals the total membrane bound transducin concentration, $\{T\text{-}GDP\}_0$. Knowing the rhodopsin surface concentration $\{R\} = 2 \times 10^4$ molecules/μm^2 and the photoexcitation level $(\{R^*\}_0/\{R\})_{sat}$ at which the binding signal saturates, one can express the transducin concentration from each sample in units of molecules/μm^2 or, more simply, relative to the total rhodopsin concentration, as $\{T\text{-}GDP\}_0/\{R\} = (\{R^*\}_0/\{R\})_{sat}$, which should be 0.1 in intact ROS because the native transducin:rhodopsin stoichiometry is 1:10 (Kühn, 1981). The saturated amplitude of the loss signal correlates well with the saturated amplitude of the binding signal from an aliquot sample (Bruckert et al., 1988); once properly calibrated it can also serve as an assay for $\{T\text{-}GDP\}_0$. Thus, the calibration factor C_{loss}, which relates the total transducin level to the maximum loss amplitude l_{max} (expressed as relative light scattering change), was obtained using saturated binding and loss signals from aliquots of ROS suspension. Evaluation from three different samples of ROS permeabilized separately gave very close estimates for C_{loss}, whose average value of

$$C_{loss} = \frac{\{T\text{-}GDP\}_0/\{R\}}{l_{max}} = \frac{(\{R^*\}_0/\{R\})_{sat}}{l_{max}} = 1.0 \pm 0.1 \qquad (5)$$

was subsequently used to evaluate the level of membrane-bound transducin in all ROS samples.

Evaluation of transducin activation from the amplitude of the release signal

The release signal is due to the activation and solubilization of Tα into the interdiscal space. The amplitude of this signal is proportional to [TαGTP], whereas its slope is proportional to $d[T\alpha GTP]/dt$, the square brackets denoting volume concentrations. As this TαGTP comes from the membrane-associated T-GDP, we can attribute to it a surface concentration $\{T\alpha GTP\}$ while keeping in mind that conversion back to a volume concentration is at any moment possible. Hence, the maximum release amplitude is also proportional to the total transducin pool on the disc surface and can be tied to saturated amplitudes of binding signals obtained from aliquots. However, the release amplitude observed must be corrected because by the time it reaches its peak, some TαGTP has already left the leaky ROS: at 100 ms when the release signal peaks, the scattering decrease due to transducin loss is already substantial (Fig. 3 *A*). If l_{peak} is the loss amplitude when the release signal reaches its peak amplitude r_{peak}, then the maximal amplitude corrected for the loss of transducin is $r_{max} = r_{peak} \times l_{max}/(l_{max} - l_{peak})$. r_{max} is used to evaluate the calibration factor $C_{release}$ that relates the saturated release amplitude to the initial transducin concentration:

$$C_{\text{release}} = \frac{\{\text{T-GDP}\}_0/\{\text{R}\}}{r_{\max}} = \frac{(\{\text{R}^*\}_0/\{\text{R}\})_{\text{sat}}}{r_{\max}} = \frac{C_{\text{loss}} I_{\max}}{r_{\max}}. \quad (5')$$

The saturated amplitudes of release and loss signals from aliquots of a given preparation of permeated ROS supplemented with increasing amounts of transducin extract always gave a consistent set of $I_{\max}/r_{\max}$ (Fig. 3 *B*). Within a preparation of ROS, one can thus obtain reproducible values for C_{release}. Between different ROS preparations, however, the value of C_{release}, seen as the slopes of the fitted lines in Fig. 3 *B*, could vary by as much as 50%. This is probably due to a poor reproducibility in the mechanical fragmentation of the ROS. Each preparation thus required a separate determination for C_{release}.

Evaluation of the velocity of transducin activation from the slope of the release signal

As alluded to above, during the rising phase of the release signal, its amplitude r is proportional to the amount of transducin released. Moreover, the maximal amplitude $r_{\max}$ corresponds to the transformation of the total pool $\{\text{T-GDP}\}_0$ of membrane-bound transducin into a soluble pool $[\text{T}\alpha\text{GTP}]_{\max}$. Thus, a slightly different form of Eq. 5 holds during the rising phase of the release signal: $\{\text{T}\alpha\text{GTP}\}/\{\text{R}\} = r \times C_{\text{release}}$. Taking its time derivative, one obtains a relation between the velocity of transducin activation and the slope of the release signal:

$$\frac{1}{\{\text{R}\}} \frac{d\{\text{T}\alpha\text{GTP}\}}{dt} = C_{\text{release}} \frac{dr}{dt}. \quad (6)$$

It is with this expression that the Michaelis-Menten relation (Eq. 1) may be applied experimentally. The requirement for steady state means that the portion of the release signal where the slope is measured has to be linear. Furthermore, the substrate concentration $\{\text{T-GDP}\}$ varies with time, strictly speaking. However, with an excess of substrate over enzyme (i.e., $\{\text{T-GDP}\}_0 \gg \{\text{R}^*\}_0$) and with steady state reached before the substrate population has significantly diminished, $\{\text{T-GDP}\}$ can be approximated by $\{\text{T-GDP}\}_0$. In our experiments, the level of photo-excitation $\{\text{R}^*\}_0/\{\text{R}\}$ was on the order of 10^{-3}, whereas the total transducin pool $\{\text{T-GDP}\}_0/\{\text{R}\}$ was always larger than 10^{-2} so that $\{\text{T-GDP}\}_0 \gg \{\text{R}^*\}_0$. The linear portion of the release signal occurred soon after the light flash, where, from the corresponding loss signal, we estimate the pool of T-GDP to be depleted by $\sim$10% only. Given these two conditions, the requirement $\{\text{T-GDP}\} = \{\text{T-GDP}\}_0$ is thus satisfied.

Transducin activation by spatially nonuniform distributions of photoexcited rhodopsin: diffusional aspects

Activating transducin with a nonuniform distribution of R* brings into play the lateral diffusion aspects of the activation process. Initial sinusoidal distributions of R* were created on the disc surface with interference fringes from two crossed laser beams (Fig. 4). The goal is to compare the kinetics of an activation due to a fringe pattern of R* with those of an activation due to a uniform R* distribution. Of course, the total amount of R* created must be identical in both cases. Three processes occur simultaneously.

(*a*) The initial sinusoidal distribution in R* relaxes to a uniform distribution with the time constant $\tau_R = L^2/4\pi^2 D_R$, where L is the fringe spacing and D_R is the lateral diffusion coefficient of rhodopsin (0.35 $\mu m^2/s$) (Fig. 4 *A*).

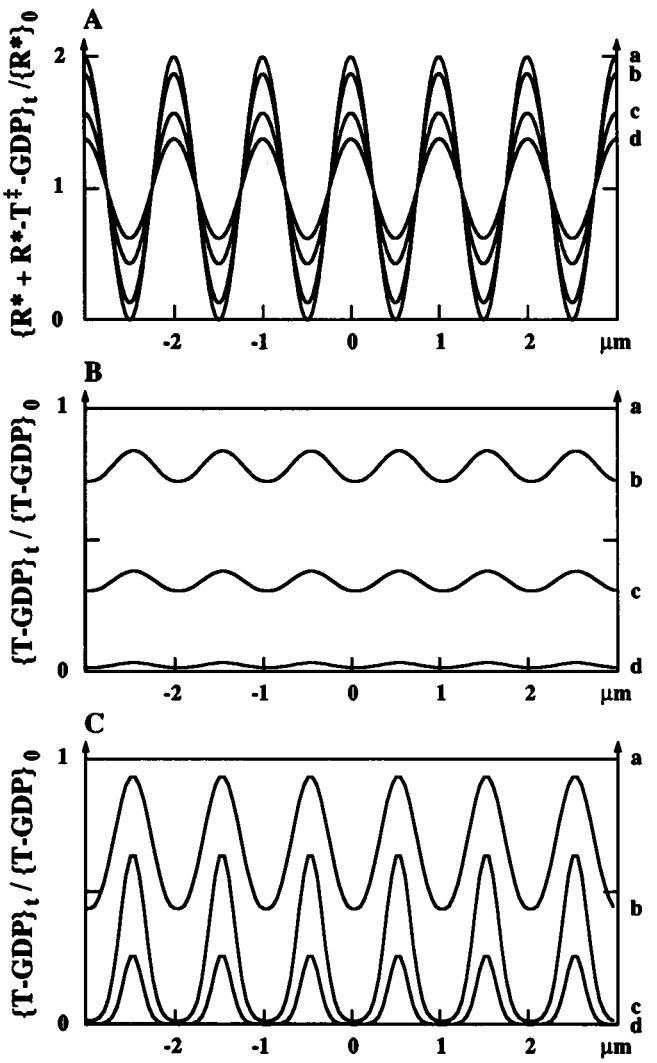

FIGURE 4 Simulated time evolution of the spatial distributions of $\{\text{R}^*\}$ and $\{\text{T-GDP}\}$ after an interference fringe flash. The simulations are performed at 0 (*a*), 10 (*b*), 40 (*c*), and 70 ms (*d*). The transducin surface concentration is set at $\{\text{T-GDP}\}_0/\{\text{R}\} = 4 \times 10^{-2}$, the catalysis time $t_{\text{cat}} = 1/k_{\text{cat}} = 1.5$ ms; the rhodopsin diffusion constant $D_R = 0.35\ \mu m^2/s$, the fringe spacing $L = 1\ \mu m$, and the rhodopsin relaxation time $\tau_R = L^2/4\pi^2 D_R = 72$ ms. (*A*) Distribution of $\{\text{R}^*\} + \{\text{R}^*\text{-T}^\ddagger\text{-GDP}\}$; the distribution at $t = 0$ (*a*) is the sinusoid with the highest contrast. (*B*) Time evolution of $\{\text{T-GDP}\}$ with $D_T = 0.05\ \mu m^2/s$ and $\{\text{R}^*\}_0/\{\text{R}\} = 3 \times 10^{-3}$; hence, $\tau_A = 90$ ms and $\tau_T = 5$ ms, i.e., $\tau_A \gg \tau_T$. From the initially uniform distribution of $\{\text{T-GDP}\}$ at $t = 0$, sinusoidal fringes of phase opposite to those of R* (see *A*) are created. Both fringe contrast and average concentration decay with time. (*C*) Same as in *B* but with $D_T = 5\ \mu m^2/s$; hence, $\tau_A = 30$ ms and $\tau_T = 500$ ms, i.e., $\tau_A \ll \tau_T$. Sinusoidal fringes are again created. They decay with time, but all along their contrast remains much larger than in *B*.

(*b*) The T-GDP molecules within the bright fringes are swiftly activated by R* and GTP, whereas those outside are relatively untouched. This results in a T-GDP stripe pattern opposite in phase to that of R*. This T-GDP pattern appears with a time constant τ_A:

$$\tau_A = \frac{1}{k_{\text{cat}}} \frac{\{\text{T-GDP}\}_0 + K_M}{\{\text{R}^*\}_0}. \quad (7)$$

τ_A is simply the inverse of the apparent rate of activation of T-GDP by R* and GTP at steady state (see Eq. 1).

(*c*) This newly created sinusoidal distribution of T-GDP in turn relaxes with the time constant $\tau_T = L^2/4\pi^2 D_T$, where D_T is the lateral diffusion coefficient of transducin.

If the lateral diffusion of R* is slow compared with the activation of transducin (i.e., $\tau_R > \tau_A$) so that the R* fringes last long enough for the T-GDP within them to be mostly activated, then the kinetics of transducin activation will depend on the relative values of τ_A and τ_T. One distinguishes two limiting cases. If transducin activation is slow compared with its diffusion, i.e., $\tau_A \gg \tau_T$, the stripe pattern of T-GDP would vanish about as fast as it is created; T-GDP will stay almost uniformly distributed on the disk, and the overall activation kinetics, which is the average of the local activation kinetics on the disk, will be relatively unchanged whether the R* distribution is uniform or sinusoidal (Fig. 4 *B*). Conversely, if transducin diffusion is slow compared with its activation, i.e., $\tau_T \gg \tau_A$, the stripe pattern of T-GDP will persist (Fig. 4 *C*). Thus, a short time after the light flash, R* and T-GDP are artificially segregated into adjacent stripes of width $L/2$. From then on the formation of TαGTP is delayed by the time it takes R* and T-GDP to diffuse over a distance $L/4$, which is $(L/4)^2/(D_R + D_T)$. With $L = 1$ μm this delay is 180 ms if $D_T = 0$ or 90 ms if $D_T = D_R = 0.35$ $\mu m^2/s$ (Poo and Cone, 1974). Such values are within the time domain of the release signal.

Compared with a uniform R* distribution, a sinusoidal distribution does not modify the total amount of T-GDP activated, because in both cases all the T-GDP is activated; the final release amplitudes are therefore identical. The initial activation rate is also not affected by a sinusoidal R* distribution because the initial T-GDP distribution is always uniform. Any changes ought to affect the intermediate kinetics only. It is the shape of the release signal that shall betray any effects due to a nonuniform photoactivation.

Mathematical modeling

To test the sensitivity of the method, we numerically simulate the temporal and spatial evolution of {R*}, {T-GDP}, and {R*-T‡-GDP} on the disc surface and from this compute the resulting activation kinetics of transducin. To simplify the boundary conditions, we treat the disc as an infinite plane. Then the computation can be limited to just one fringe of width $L = 1$ μm (Fig. 4). We again use the reaction scheme of Fig. 1 *B*, which involves three species that diffuse laterally on the disk membrane: R*, T-GDP, and R*-T‡-GDP. The three coupled partial differential equations are:

$$\frac{\partial\{R^*\}}{\partial t} = D_R \frac{\partial^2\{R^*\}}{\partial x^2} - k_{on}\{R^*\}\{\text{T-GDP}\} + k_{cat}\{R^*\text{-T}^\ddagger\text{-GDP}\}$$

$$\frac{\partial\{R^*\text{-T}^\ddagger\text{-GDP}\}}{\partial t} = D_R \frac{\partial^2\{R^*\text{-T}^\ddagger\text{-GDP}\}}{\partial x^2} + k_{on}\{R^*\}\{\text{T-GDP}\} - k_{cat}\{R^*\text{-T}^\ddagger\text{-GDP}\}$$

$$\frac{\partial\{\text{T-GDP}\}}{\partial t} = D_T \frac{\partial^2\{\text{T-GDP}\}}{\partial x^2} - k_{on}\{R^*\}\{\text{T-GDP}\}$$

where the fringe spacing L is 1 μm, x is the spatial position, and t is the time after the flash so that $0 < x < L$ and $t > 0$.

The boundary conditions are:

$$\frac{\partial\{R^*\}}{\partial x} = \frac{\partial\{R^*\text{-T}^\ddagger\text{-GDP}\}}{\partial x} = \frac{\partial\{\text{T-GDP}\}}{\partial x} = 0$$

at $x = 0$ and $x = L$, for every t.

The initial conditions are:

$$\{R^*\}(x, t = 0) = \{R^*\}_0\left(1 + m \cdot \cos\left(\frac{2\pi x}{L}\right)\right)$$

with $m = 0$ for uniform photoexcitation and $m = 1$ for fringe photoexcitation.

$$\{R^*\text{-T}^\ddagger\text{-GDP}\}(x, t = 0) = 0$$
$$\{\text{T-GDP}\}(x, t = 0) = \{\text{T-GDP}\}_0.$$

At any time t, the amount of TαGTP produced is given by:

$$\{T\alpha GTP\}(t) = \int_0^L (\{\text{T-GDP}\}_t - \{\text{T-GDP}\}(x, t) - \{R^*\text{-T}^\ddagger\text{-GDP}\}(x, t))\, dx.$$

The same diffusion coefficient D_R is used for both R* and the complex R*-T‡-GDP.

Numerical simulation

The above partial differential equations were solved numerically using a method described by Churchhouse (1981). We focus here on the results, i.e., on the simulated activation kinetics of transducin as they are influenced by various parameters. The difference between the activation kinetics obtained with uniform photoexcitation and those obtained with fringe photoexcitation is shown in Fig. 5.

(*a*) Influences of the photoexcitation level and the total transducin pool $\{\text{T-GDP}\}_0$. The photoexcitation level $\{R^*\}_0/\{R\}$ is critical because if the T-GDP activation rate is too low, the T-GDP fringes will disappear almost as fast as they are created, and the fringe-induced activation kinetics will differ little from those due to uniform illumination. The simulation shows that $\{R^*\}_0/\{R\}$ should be higher than 2×10^{-3} (Fig. 5 *B*). However, the slope of the release signal starts saturating with R*/R above 5×10^{-3}, so that a useful range of R*/R should be $\sim 2\text{–}5 \times 10^{-3}$. In contrast, within the concentration range observed, the size of the initial transducin pool, $\{\text{T-GDP}\}_0/\{R\}$, is not a very sensitive parameter; varying $\{\text{T-GDP}\}_0/\{R\}$ from 2 to 5×10^{-2} did not change the difference curve between uniform and sinusoidal illumination by >10% (data not shown). As will be seen, this is because the Michaelis constant K_M is significantly below this concentration range. Lower levels of $\{\text{T-GDP}\}_0/\{R\}$ should give more pronounced differences but the release signals become too small to be accurately measured.

(*b*) Influence of the diffusion coefficient D_T of transducin. Setting D_R constant at 0.35 $\mu m^2/s$ and varying D_T between 0.035 and 1.75 $\mu m^2/s$, one sees clearly that the difference between uniform and sinusoidal illumination grows as the ratio D_T/D_R increases from 0.1 to 5, that is, as transducin is made to diffuse slower compared with rhodopsin (Fig. 5 *C*). However, the maximum difference obtained is only $\sim 10\%$.

(*c*) Effect of the uncertainty in the reported value for D_R. An increase of D_R would result in a faster disappearance of the R* fringes, thus reducing the difference in activation kinetics between sinusoidal and uniform illuminations. Keeping D_T constant at a value of 0.035 or 1.75 $\mu m^2/s$ and varying D_R between its lower and upper bounds of 0.2 and 0.5 $\mu m^2/s$, one observes that the activation kinetics are pretty much unmodified (Fig. 5 *D*). This indicates that the precision with which D_R is reported is sufficient for these computations.

(*d*) Effect of the uncertainty in the catalysis time $t_{cat} = 1/k_{cat}$. As can be seen from Eq. 6, at some level of $\{R^*\}_0$, a longer catalysis time t_{cat} would result in a larger value for τ_A: the appearance of the T-GDP would be delayed. At the $\{R^*\}_0$ level suggested by the simulation in Fig. 5 *A*, what is the effect of changing t_{cat} in the range of values suggested by previous work (Vuong et al., 1984)? As can be seen in Fig. 5 *E*, two dissimilar values of t_{cat} give rise to curves whose difference in shape would be easily measurable.

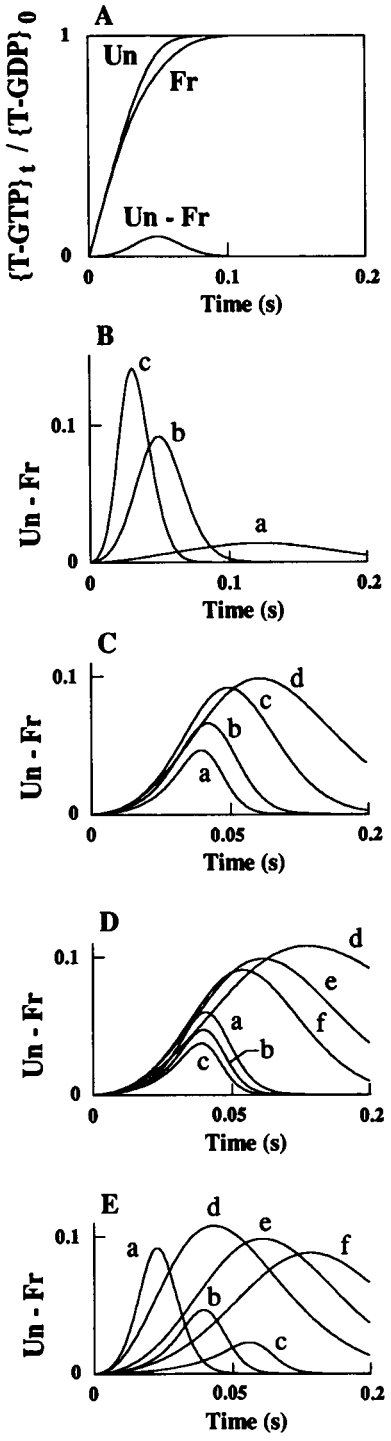

FIGURE 5 Simulation of the effects of fringe illumination on the kinetics of transducin activation. The fractions of transducin activated, $\{T\alpha GTP\}/\{T\text{-}GDP\}_0$, are plotted as functions of time, because they would be observed via release signals elicited by uniform (Un) or fringe (Fr) flashes of identical intensities. The difference Un − Fr is a measure of how much a sinusoid pattern of illumination affects the activation kinetics. (*A*) $\{R^*\}_0/\{R\} = 3 \times 10^{-3}$; transducin concentration $\{T\text{-}GDP\}_0/\{R\} = 5 \times 10^{-2}$; diffusion coefficients $D_R = 0.35\ \mu m^2/s$; $D_T = 0.35\ \mu m^2/s$; catalysis time $t_{cat} = 1/k_{cat} = 2$ ms. (*B*) Dependence of Un − Fr on the photoexcitation levels: $\{R^*\}_0/\{R\} = 10^{-3}$ (*a*), 3×10^{-3} (*b*) (same as in *A*) and 5×10^{-3} (*c*). (*C*) Dependence of Un − Fr on the diffusion coefficient of transducin: $D_T = 0.035$, 0.35, 1.05, and 1.75 $\mu m^2/s$ in *a*, *b*, *c*, and *d*, respectively. (*D*) Sensitivity of Un − Fr on the value of D_R. Simulation performed with two different values of D_T: 1.75 $\mu m^2/s$ (*a*, *b*, and *c*) or 0.035 $\mu m^2/s$ (*d*, *e*, and *f*), with $D_R = 0.2$ $\mu m^2/s$ (*a* and *d*), 0.35 $\mu m^2/s$ (*b* and *e*), and 0.5 $\mu m^2/s$ (*c* and *f*). (*E*) Dependence of Un − Fr on the catalysis time $t_{cat} = 1/k_{cat}$. Simulations performed with two different values of D_T: 1.75 $\mu m^2/s$ (*a*, *b*, and *c*) or 0.035 $\mu m^2/s$ (*d*, *e*, and *f*), with $t_{cat} = 1$ ms (*a* and *d*), 2 ms (*b* and *e*), and 3 ms (*c* and *f*).

RESULTS

Estimation of k_{cat} and K_M for the activation of transducin by R* at saturating GTP level

The kinetic parameters for the steady-state activation of transducin by R* were obtained by analyzing the amplitude and slopes of the release and loss signals from oriented ROS samples. Illumination by the photographic flash was spatially uniform, and the GTP levels were saturating (see Materials and Methods). Each sample consisted of a series of aliquots to which increasing amounts of crude transducin extract were added. The surface concentration of transducin, $\{T\text{-}GDP\}_0/\{R\}$, for each aliquot was evaluated (Eq. 5) from the saturated amplitude of the loss signal ($R^*/R = 4 \times 10^{-4}$). Moreover, a value for $C_{release}$ was computed for each series of aliquots from the corresponding saturated release and loss amplitudes (Eq. 5′). The steady-state rate of transducin activation was then obtained from the slope of a subsaturated ($R^*/R = 1.3 \times 10^{-4}$) release signal (Eq. 6).

Figure 6 shows a typical series of measurements. With more and more transducin extract added to the ROS suspension, the membrane-bound T-GDP concentration as measured by the loss and release amplitudes increased about sixfold. In contrast, the transducin activation velocity as measured from the maximal slope of the release signal saturated after having increased about threefold. The result of all our measurements are combined in Fig. 7, where the activation velocity is plotted as a function of transducin surface concentration. These measurements were done at concentration of GTP varying from 400 to 1,500 μM. The resulting data show little variation, suggesting that k_{cat} is already saturated at 400 mM GTP. Values of $k_{cat} = 8 \pm 1 \times 10^2\ s^{-1}$ and $K_M/\{R\} = 2 \pm 0.4\ 10^{-2}$ were extracted from a nonlinear least-square fit of the data points to the Michaelis-Menten relation (Eq. 1). The uncertainties include three main contributions: (*a*) the dispersion of the data points, (*b*) the uncertainty in the calibration factors C_{loss} and $C_{release}$, and (*c*) the uncertainty in the photoexcitation level $\{R^*\}_0/\{R\}$, which also affects C_{loss} and $C_{release}$ through the determination of the saturating level $(\{R^*\}_0/\{R\})_{sat}$. In the absence of GDP, the minimum catalysis time t_{min} taken by R* to activate transducin (Eq. 4) is $t_{min} = 1/k_{cat} = 1.2 \pm 0.2 \times 10^{-3}$ s. As the total

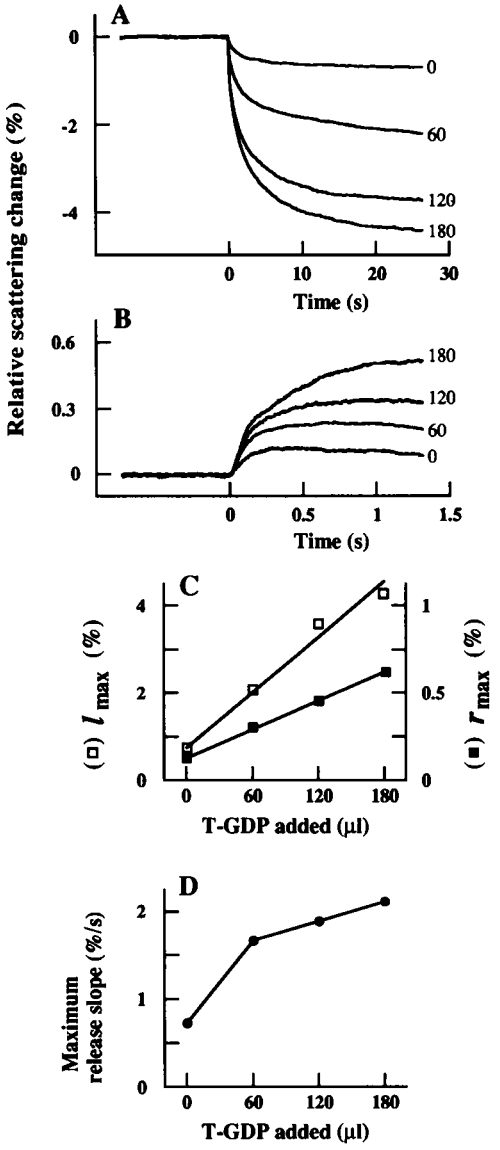

FIGURE 6 Supplementing a ROS suspension with exogenous transducin affects the amplitude and kinetics of the release and loss signals (uniform flashes). Membrane concentration = 1.7 μM rhodopsin, [GTP] = 0.77 mM, 21°C. The transducin extract (860 μl) was from 18 retinas. (*A*) Loss signals after a saturating flash ($\{R^*\}_0/\{R\} = 4 \times 10^{-3}$); the amount of transducin extract added increased from 0 to 180 μl. (*B*) Release signals observed after a nonsaturating flash ($\{R^*\}_0/\{R\} = 10^{-3}$) on aliquots of the same samples. (*C*) Evolution of the amplitude of the loss signals I_{max} (□), of the release signal r_{max} (■), and of the maximal slope of the release signal (●). These plots demonstrate the linearity of the amplitudes of the loss signal and release signal with the amount of added transducin extract, and by contrast, the saturation of the slope of the release signal.

concentration of rhodopsin on the disk, {R} is (2.0 ± 0.2) × 10^4 molecules/μm² (Chabre, 1985; Liebman et al., 1987), we obtain k_{cat}/K_M = 2.0 ± 0.5 μm²/s. In situ where total concentration of transducin, {T-GDP}$_0$, is about one-tenth of the total concentration of rhodopsin, {R}, the time t_{form} (Eq. 3) taken to form the enzyme-substrate complex would be t_{form} = 0.25 ± 0.1 × 10^{-3} s.

Influence of added GDP on the rate of transducin activation: estimation of k_{+GTP} and k_{+GDP}

GDP might compete with GTP for the nucleotide site of an R*-bound transducin and thus interfere with the process of transducin activation (see Materials and Methods). To search for this effect, up to 1 mM GDP was added to ROS aliquots containing 0.5 mM GTP; the photoexcitation level was sufficient to elicit total activation of transducin in the GDP-free control aliquot (Fig. 8). From the affinities of GTP and GDP for Mg^{2+}, 0.1 and 0.4 mM, respectively (Martell and Smith, 1976), and the amount of $MgCl_2$ added (2.1 mM), we estimate that with 0.5 mM GTP alone, the free [Mg^{2+}] is 1.6 mM and with 1 mM GDP added, it drops to 0.9 mM. This range of free Mg^{2+} is well within reason; activation of transducin by R* requires ~0.1 mM free Mg^{2+}, whereas a spontaneous dissociation of TαGDP from Tβγ only occurs at ~10 mM Mg^{2+} (Deterre et al., 1984). The added GDP had little effect on the release and loss amplitudes, but the slope of the release signal decreased by a factor of 2. The longer time needed for the release signal to peak when exogenous GDP was present can entirely account for its slightly lower amplitude; that much more transducin is lost during this extra delay (see Materials and Methods and Fig. 3 *A*). The amount of transducin activated by the flash was therefore not affected by the added GDP. But the rate of transducin activation as deduced from the slope of the release signal decreased linearly as the [GDP]/[GTP] ratio increased (Fig. 8 *C*). The kinetic consequence of this competition between

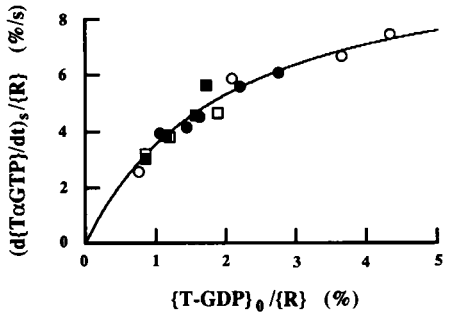

FIGURE 7 Dependence of the activation rate of transducin after a flash on the initial surface concentration of transducin. The transducin concentration was varied by addition of varying amounts of transducin extracts to aliquots of ROS suspension. The initial surface concentration, $\{T\text{-}GDP\}_0/\{R\}$, was assayed in each sample using the amplitude of a saturated loss signal (Eq. 5). The steady-state activation velocity of transducin, $(1/\{R\})\cdot(d\{T\alpha GTP\}/dt)_s$, was obtained from the slope of the release signal (Eq. 4'), using a calibration factor $C_{release}$ determined as in Fig. 3. The different sets of points represent data from different ROS samples. Membrane concentration = 1.7 μM rhodopsin for all samples; 21 ± 1°C; $\{R^*\}_0/\{R\} = 1.3 \times 10^{-4}$; GTP concentrations between 0.4 and 1.5 mM (see text). The data were fitted to the Michaelis-Menten equation (Eq. 1) by a nonlinear least-square procedure, which yielded k_{cat} = 8 ± 1 × 10^2 s^{-1} and $K_M/\{R\}$ = 2 ± 0.4 × 10^{-2}.

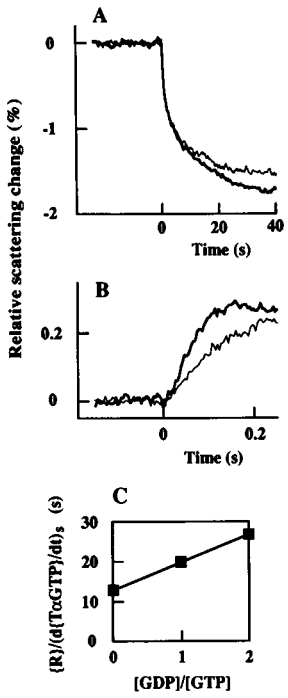

FIGURE 8 Influence of free GDP concentration on the rate of transducin activation. (*A*) Loss signals from ROS aliquots containing 0.5 mM GTP and supplemented (thin trace) or not (thick trace) with 1 mM GDP; R*/R = 3.8×10^{-4}; membrane concentration = 2.5 μM rhodopsin. The amplitudes of the signals are not significantly affected by addition of GDP. (*B*) Release signals. Addition of GDP significantly slows down the rising phase of the signal, resulting in a slightly lower value for r_{peak} (see Fig. 3). (*C*) Dependence of the transducin steady-state activation rate on the [GDP]/[GTP] ratio.

GDP and GTP for the empty nucleotide site is a delay in the binding of GTP and hence a slow down in transducin activation. This effect is described by Eqs. 4 and 4'. Putting into Eq. 4' the value of $K_M/\{R\} = 2.0 \pm 0.4 \times 10^{-2}$ as determined above and the reported value of 20 ± 10 μM for K_{GDP} (Bennett and Dupont, 1985), we obtain $k_{+GTP} = 4.2 \pm 2.4 \times 10^7\ M^{-1}\ s^{-1}$. Using this value of k_{+GTP} in Eq. 3, we estimate that with GDP and GTP added in equal amounts, catalysis is lengthened by 1.2 ms. This is roughly equal to the minimum catalysis time t_{min}; raising the GDP level to about that of GTP doubles the time it takes R* to catalyze the activation of transducin. How does k_{+GDP} compare with k_{+GTP}? From the expressions for t_{min}, the definition of K_{GDP} and the numerical values for t_{min} and K_{GDP}, the following inequalities are obtained:

$$t_{min} > t_{GDP} = \frac{1}{k_{-GDP}} = \frac{1}{K_{GDP} k_{+GDP}} \Rightarrow$$

$$k_{+GDP} > \frac{1}{t_{min} K_{GDP}} = 4.1 \pm 2.1 \times 10^7\ M^{-1}\ s^{-1}.$$

Thus, the entry of GDP into the open nucleotide site of an R*-bound transducin is at least as rapid as that of GTP.

A lower bound for the lateral diffusion coefficient of transducin from the steady-state kinetics

The ratio k_{cat}/K_m is a lower bound for k_{form}, the rate constant for the formation of the R*-T*-GDP complex, itself a lower bound for the encounter rate constant k_{+enc} between R* and T-GDP (see Materials and Methods). This encounter rate k_{+enc} can be related to the diffusion coefficients D_R and D_T of R* and T-GDP through an expression by Berg and Purcell (1977):

$$k_{+enc} = \frac{2\pi(D_R + D_T)}{\ln(b/a) - 3/4} > \frac{k_{cat}}{K_M}$$

where a is the sum of the radii of R* and T-GDP and b is half the mean distance between neighboring R*. Using a diameter of 30 Å for rhodopsin (Osborne et al., 1978) and assuming that T-GDP is a sphere of density 1.4, we obtain a = 45 Å; b depends on the total concentration $\{R^*\}_0$ on the disks: $b = 1/\sqrt{\pi\{R^*\}_0}$ = 3,500 Å. These values lead to $D_R + D_T > 1.2 \pm 0.3$ $\mu m^2/s$, where the uncertainty is from the value of k_{cat}/K_M. Since $D_R = 0.35 \pm 0.15$ $\mu m^2/s$ (Poo and Cone, 1974), the lower bound for the lateral diffusion coefficient D_T for transducin is $D_T > 0.8 \pm 0.5$ $\mu m^2/s$. This means that transducin diffuses laterally at least as fast as rhodopsin and most likely much faster.

Search for an effect of nonuniform photoexcitation by laser interference fringes on the kinetics of transducin activation

The release signals elicited by fringe interference flashes were compared with those elicited by uniform flashes of equal intensity on aliquots of a ROS suspension. Figure 9 shows the results of four such complete experiments on four different ROS samples. Each experiment consisted of measurements on eight aliquots, four of which were illuminated with interference fringes, whereas the other four served as controls, where R* was uniformly created by illumination with only one of the two split beams but of doubled intensity (see Materials and Methods). The two split beams were used alternatingly to illuminate the four control aliquots. The order in which the eight aliquots were illuminated was scrambled so as to minimize any bias due to sample aging during the full duration of each experiment, which lasted no longer than 2 h. The four recordings for each type of illumination were summed up. The photoexcitation level R*/R was varied from 2 to 4×10^{-3}, these values being selected on the basis of the numerical simulation described in Materials and Methods. The ROS suspensions (0.38 μM rhodopsin) were supplemented with crude transducin extracts, and the loss component of the signals was used to assay for the transducin surface concentration $\{T\text{-}GDP\}_0/\{R\}$ that ranged from 1.9 to 4×10^{-2}.

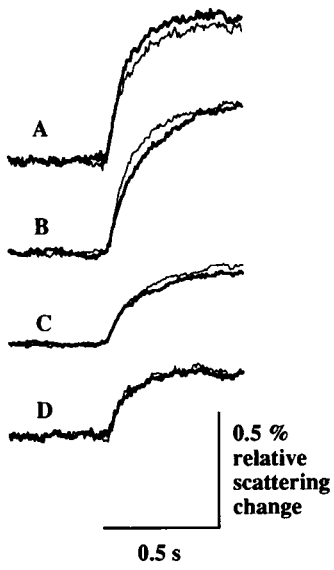

FIGURE 9 Looking for an influence of nonuniform distributions of R* on the activation kinetics of transducin. Comparison of release signals elicited by uniform flashes (thick traces) or interference fringe flashes (thin traces) of identical intensities on pairs of ROS aliquots (membrane concentration = 0.35 μM rhodopsin) supplemented with various amounts of transducin. (*A*) $\{R^*\}_0/\{R\} = 4 \times 10^{-3}$, surface transducin concentration $\{\text{T-GDP}\}_0/\{R\} = 4.0 \times 10^{-2}$. (*B*) $\{R^*\}_0/\{R\} = 2 \times 10^{-3}$, $\{\text{T-GDP}\}_0/\{R\} = 3.5 \times 10^{-2}$. (*C*) $\{R^*\}_0/\{R\} = 2 \times 10^{-3}$, $\{\text{T-GDP}\}_0/\{R\} = 1.9 \times 10^{-2}$ (*D*) $\{R^*\}_0/\{R\} = 2 \times 10^{-3}$, $\{\text{T-GDP}\}_0/\{R\} = 2.5 \times 10^{-2}$. The surface transducin concentrations were estimated from the amplitude of the corresponding loss signals (Eq. 5).

As seen in Fig. 9, the amplitudes of the release signals are very similar for the two types of illuminations. Thus, the average intensity of fringe illumination is equal to that of the uniform flash. Summation over four aliquots notwithstanding, there remains a significant level of noise in the traces. Given the very low ROS concentration, this noise is most likely due to statistical fluctuation of the number of rods in the infrared light beam. Because of this limited accuracy, the small differences observed are not significant. Indeed, in the second set of recordings, the kinetics due to fringe illumination appear slightly faster than those due to uniform illumination, a difference that cannot be real. In the current experimental context, we cannot detect any significant kinetic differences between release signals elicited with sinusoidal or uniform distributions of R*.

The absence of a measurable delay in the activation of transducin when the pattern of R* on the disc is sinusoidal suggests that the characteristics time τ_A (Eq. 7) with which R* activates transducin is larger than the time τ_T taken by the transducin fringes to disappear. That is:

$$\frac{L^2}{4\pi^2 D_T} < \frac{1}{k_{cat}} \frac{\{\text{T-GDP}\}_0 + K_M}{\{R^*\}_0}.$$

With $L = 1$ μm, $\{\text{T-GDP}\}_0/\{R\} \approx 3 \times 10^{-2}$, $\{R^*\}_0/\{R\} \approx 3 \times 10^{-3}$ (Fig. 8), $k_{cat} = 800\ s^{-1}$, and $K_m/\{R\} = 2 \times 10^{-2}$ (from the steady-state analysis), we obtain $D_T > 1.2\ \mu m^2/s$. This estimate for the lower bound of the lateral diffusion coefficient of transducin agrees well with that obtained above from the steady-state Michaelis-Menten analysis.

DISCUSSION

We have used the light scattering release signal (Vuong et al., 1984) as a monitor to kinetically dissect the activation of transducin by photoexcited rhodopsin. The study aimed at addressing two questions: is the activation of transducin by R* limited by the lateral diffusion of the two molecules and does the presence of a high level of GDP have any effects on the kinetics of activation? Because several previous studies (Bennett and Dupont, 1985; Bornancin et al., 1989) had suggested that the empty nucleotide site on the R*-T_{empty} complex is equally accessible to both GDP and GTP, one must suspect there is competition from both, giving rise to a slow down in the activation rate.

On the one hand, the classic Michaelis-Menten formalism was applied to this activation process with R* as enzyme and T-GDP as substrate. The substrate level was varied by addition of exogenous transducin and its surface concentration assayed by a concerted use of the light scattering binding and loss signals (Bruckert et al., 1988). Much could be learned about the kinetics of transducin activation from the catalysis and Michaelis constants, k_{cat} and K_M, obtained from this classical treatment. On the other hand, the technique of laser interference fringes was applied to create a nonuniform distribution of R* on the disk surface and to see what effects this has on the activation rate as monitored by the release signal.

Activation of transducin by R* is not limited by lateral diffusion

Of the time taken by one R* to activate one transducin, how much is taken up by the process of catalysis itself and how much by the formation of the enzyme-substrate complex, a process that depends at least in part on the lateral diffusion of R* and transducin? In the absence of GDP and at saturating levels of GTP, one obtains the shortest catalysis time of 1.2 ms; there is significant lengthening of this time when [GDP] is about equal to [GTP]. Assuming an in vivo rhodopsin:transducin stoichiometry of 10:1, the enzyme-substrate formation time is only 0.25 ms. At most, it takes but 20% of the total activation time for R* and T-GDP to meet by lateral diffusion and to form the complex R*-T‡-GDP. From this consideration alone, we can already say that the process of lateral diffusion does not play a predominant role in the activation of transducin by R*.

From the value of k_{cat}/K_M, a lower bound for the lateral diffusion coefficient of transducin is estimated to be

$\sim$0.8 $\mu m^2/s$; transducin diffuses laterally at least as fast as rhodopsin and probably much faster. This finding dovetails with what is said above: activation of transducin by R* is not determined kinetically by lateral diffusion.

Finally, the kinetics of the release signal are apparently not influenced by the way R* is spatially distributed on the disk surface; uniform or sinusoidal patterns of R* elicited signals of very similar kinetics. However, given the low precision of these measurements, we can only say they are not inconsistent with the notion that R* and transducin diffuse fast enough for the formation step to contribute little to the overall time of activation.

Kahlert and Hofmann (1991) used the light scattering "ATR" signal from intact retinas (Pepperberg et al., 1988) to study the collisional efficiency of the R*-transducin association in intact bovine retinas. The ATR signal is similar to our release signal because they both arise from the solubilization of TαGTP into the interdiscal space. Assuming a value of 1 $\mu m^2/s$ for the lateral diffusion coefficient of transducin, these authors computed a theoretical encounter rate between R* and transducin (using the equation of Berg and Purcell, 1977) and compared it with a rate of R*-transducin association deduced from the measured ATR signals. From this comparison, a collisional efficiency of $\sim$30% was obtained. This low value might lead one to conclude that the activation of transducin by R* is limited by lateral diffusion. Such interpretation, however, would be unjustified. The problem is mainly one of definition: "Success of a collision is understood as formation of an MII-G (R*-T in our notation) complex with an accessible nucleotide binding site which allows entry of the activating cofactor GTP" (Kahlert and Hofmann, 1991). Thus, these authors include in the formation of the enzyme-substrate complex the opening of the nucleotide site on transducin and the departure of GDP from this site. Moreover, they also lumped in the dissociation of TαGTP from R*. In fact, the only chemistry they considered separately was the entry of GTP into the empty nucleotide site. Hence, most of the chemistry of catalysis was mixed up with the diffusional process by which R* and transducin meet. It is therefore no wonder that once comparison was made with the strictly diffusion-related rate of Berg and Purcell, the efficiency obtained was so low.

Our measurement of k_{cat}/K_M indicates that the lateral diffusion coefficient of transducin is on the order of 1 $\mu m^2/s$, assuming all collisions are successful. We define as successful those collisions that result in a complex R*-T‡-GDP where little of the chemistry of catalysis has occurred. The only chemistry considered at this stage is the conformational change from the strictly inactive, unpartnered T-GDP form to the R*-bound form, T‡-GDP; much remains to be done before TαGTP appears in the interdiscal space to give rise to the observable release signal. The mobility of 0.35 $\mu m^2/s$ for rhodopsin is very high for an integral membrane protein in its physiological bilayer and as such has been thought necessary for a fast activation of transducin. Our result does not support such hypothesis; transducin diffuses sufficiently fast that a lower rhodopsin mobility should not adversely affect the kinetics of activation. Indeed, it is remarkable that squid rhodopsin is immobilized by linkage to the cytoskeleton (Saibil, 1982); it seems lateral diffusion of rhodopsin is not even required for an efficient phototransducin cascade.

A value of $\sim$1 $\mu m^2/s$ for the lateral mobility of transducin is similar to that of most peripheral membrane proteins. Indeed, proteins such as Band 4.1 (Chang et al., 1981), spectrin (Chang et al., 1981), apolipo-protein CIII (Vaz et al., 1979), and an antibody linked to a lipid hapten (Smith et al., 1979) all have mobilities in the range 0.9–4.2 $\mu m^2/s$. Using the protein Band 4.1 as a benchmark, Saxton and Owicki (1989) predicted a range of 0.7–2.7 $\mu m^2/s$ for the diffusion coefficient of transducin.

Competition between GDP and GTP for the open nucleotide site contributes substantially to the kinetics of activation in vivo

Our results show that GDP competes effectively against GTP for the open, empty nucleotide site of the α-subunit of transducin: at 0.5 mM GTP, 1 mM GDP halved the maximum slope of the release signal. Kahlert et al. (1990) reported a much lower level of competition; at 0.02 mM GTP, 0.15 mM GDP was needed to halve the loss component of the dissociation signal. However, this apparently lesser competition is probably due to the very low level of GTP used. Within the narrow interdiscal space, the local concentration of the endogenous GDP released by transducin upon interaction with R* would be comparable with the low level of GTP present. Most of the deceleration effect GDP has on the kinetics would already occur, and any additional influence from the exogenous GDP would be slight.

To put this GDP effect on firmer quantitative grounds, we needed to measure the bimolecular rate constant for the entry of GTP into the nucleotide site (Eq. 4): $k_{+GTP} = 4.2 \pm 2.4 \times 10^7\ M^{-1}\ s^{-1}$, the substantial uncertainty being mainly due to the imprecise value of the affinity K_{GDP}. From the report of Kohl and Hofmann (1987), one can deduce a similar value of $10^7\ M^{-1}\ s^{-1}$ for k_{+GTP}. At 20°C, k_{+GTP} is thus about an order of magnitude below the diffusion limit of $5 \times 10^8\ M^{-1}\ s^{-1}$; this is pretty much the norm for most small molecules that interact with proteins (Fersht, 1985). In the absence of GDP, the entry of GTP becomes limiting when $1/k_{+GTP}[GTP] \geq t_{min}$ (Eq. 4), giving a K_{50} for GTP of 20 μM. This is far below the millimolar range of GTP concentrations in vivo (Robinson and Hagins, 1979; Biernbaum and Bownds, 1985), meaning that physiologically the entry of GTP contributes little to the activation time of transducin.

As GDP is seen to slow down the kinetics of transducin activation, a pertinent question to ask is, just how much GDP is there in an intact retinal rod cell? Robinson and Hagins (1979) reported 2.5 mM GDP and 2 mM GTP in freshly separated ROS; de Azaredo et al. (1981) reported 1 mM GDP and 2 mM GTP in the intact rods of retinas. From these values, we estimate (Eqs. 3 and 4) that the delay due to competition by GDP takes up from 25 to 50% of the total activation time. Thus, if there was a rate-limiting process in the activation of transducin by R*, a likely candidate would be this process of nucleotide exchange, given the existence of this GDP competition effect and the presence of rather high levels of GDP in vivo.

Received for publication 2 January 1992 and in final form 30 April 1992.

REFERENCES

Baylor, D. A., B. J. Nunn, and J. L. Schnap. 1984. The photocurrent, noise and spectral sensitivity of rod of the monkey *Macaca fascicularis*. *J. Physiol. (Lond.)*. 357:575–607.

Bennett, N., and Y. Dupont. 1985. The G-protein of retinal rod outer segments (transducin): mechanism of interaction with rhodopsin and nucleotides. *J. Biol. Chem.* 360:4156–4168.

Berg, H. C., and E. M. Purcell. 1977. Physics of chemoreception. *Biophys. J.* 20:193–219.

Biernbaum, M. S., and M. D. Bownds. 1985. Light induced changes in GTP and ATP in frog rod photoreceptors. *J. Gen. Physiol.* 85:107–121.

Bornancin, F., C. Pfister, and M. Chabre. 1989. The transition state complex between photoexcited rhodopsin and transducin. *Eur. J. Biochem.* 14:687–698.

Bruckert, F., T. M. Vuong, and M. Chabre. 1988. Light and GTP dependence of transducin solubility in retinal rods: further analysis by near infrared light scattering. *Eur. Biophys. J.* 16:207–218.

Chabre, M. 1975. X-ray diffraction studies on retinal rods. I. Structure of the disk membrane, effect of illumination. *Biochim. Biophys. Acta.* 382:322–335.

Chabre, M. 1985. Trigger and amplification mechanisms in visual phototransduction. *Annu. Rev. Biophys. Biophys. Chem.* 14:331–360.

Chang, C. H., H. Takeuchi, T. Ito, K. Machida, and S. Ohnishi. 1981. Lateral mobility of erythrocyte membrane proteins studied by the fluorescence photobleaching recovery technique. *J. Biochem. (Tokyo)*. 90:997–1004.

Churchhouse, R. F. 1981. Handbook of Applicable Mathematics. Vol. III. Numerical Methods. John Wiley & Sons, Inc., Chichester, UK. 565 pp.

De Azerado F. A. M., W. D. Lust, and J. V. Passoneau. 1981. Light induced change in energy metabolites, guanine nucleotide and guanylate cyclase within frog retinal layer. *J. Biol. Chem.* 256:2731–2735.

Deterre, P., J. Bigay, C. Pfister, and M. Chabre. 1984. Guanine nucleotides and magnesium dependence of the association states of the subunits of transducin. *FEBS (Fed. Eur. Biochem. Soc.) Lett.* 178:228–231.

Fersht, A. 1985. Enzyme Structure and Mechanism. W. H. Freeman, New York. 475 pp.

Kahlert, M., and K. P. Hofmann. 1991. Reaction rate and collision efficiency of the rhodopsin-transducin system in the intact retinal rod. *Biophys. J.* 59:375–386.

Kahlert, M., B. König, and K. P. Hofmann. 1990. Displacement of rhodopsin by GDP from the three loop interaction with rhodopsin depends critically on the diphosphate β position. *J. Biol. Chem.* 265:18928–18932.

Kohl, B., and K. P. Hofmann. 1987. Temperature dependence of G-protein activation in photoreceptor membranes. Transient extra Meta-II on bovine disk membranes. *Biophys. J.* 52:271–277.

Kühn, H. 1981. Interaction of rod cell proteins with the disk membrane: influence of light, ionic strength and nucleotides. *Curr. Top. Membr. Transp.* 15:171–201.

Liebman, P. A., and A. Sitaramayya. 1984. Role of G-protein-receptor interaction in amplified phosphodiesterase activation of retinal rods. *Adv. Cyclic Nucleotide Protein Phosphorylation Res.* 17:215–225.

Liebman, P. A., K. R. Parker, and A. Dratz. 1987. The molecular mechanisms of visual excitation and its relation to the structure and composition of the rod outer segment. *Annu. Rev. Physiol.* 49:765–791.

Martell, A. F., and R. M. Smith. 1976. Critical Stability Constant. Vol. 2. Plenum Press, New York. 780 pp.

Osborne, H. B., C. Sardet, M. Michel-Villaz, and M. Chabre. 1978. Structural study of rhodopsin in detergent micelles by small angle neutron scattering. *J. Mol. Biol.* 123:177–206.

Pepperberg, D. R., M. Kahlert, A. Krause, and K. P. Hofmann. 1988. Photic modulation of a highly sensitive, near infra-red light-scattering signal recorded from intact retinal photoreceptors. *Proc. Natl. Acad. Sci. USA.* 85:5531–5535.

Poo, M., and R. A. Cone. 1974. Lateral diffusion of rhodopsin in the photoreceptor membrane. *Nature (Lond.)*. 247:441.

Robinson, W. E., and W. A. Hagins. 1979. GTP hydrolysis in intact rod outer segments and the transmitter cycle in visual excitation. *Nature (Lond.)*. 280:398–400.

Saibil, H. R. 1982. An ordered membrane-cytosqueletton network in squid photoreceptor microvilli. *J. Mol. Biol.* 158:435–456.

Saxton, M. J., and J. C. Owicki. 1989. Concentration effects on reactions in membranes: rhodopsin and transducin. *Biochim. Biophys. Acta.* 979:27–34.

Schleicher, A., and K.-P. Hofmann. 1987. Kinetic study on the equilibrium between membrane bound and free photoreceptor G-protein. *J. Membr. Biol.* 95:271–281.

Smith, L. M., J. W. Parce, B. A. Smith, and H. M. McConnell. 1979. Antibodies bound to lipid haptens in model membranes diffuse as fast as the lipids themselves. *Proc. Natl. Acad. Sci. USA.* 76:4177–4179.

Stryer, L. 1986. Cyclic GMP cascade of vision. *Annu. Rev. Neurosci.* 9:87–119.

Vaz, W. L. C., K. Jacobson, E. S. Wu, and Z. Derkzo. 1979. Lateral mobility of an amphopathic apolipoprotein, ApoC-III, bound to phosphatidylcholine bilayers with and without cholesterol. *Proc. Natl. Acad. Sci. USA.* 76:5645–5649.

Vuong, T. M. 1984. Kinetic studies of the activation of transducin by photoexcited rhodopsin. Ph.D. thesis. Stanford University, Stanford, CA. 101 pp.

Vuong, T. M., M. Chabre, and L. Stryer. 1984. Millisecond activation of transducin in the cyclic nucleotide cascade of vision. *Nature (Lond.)*. 311:659–661.

Zimmermann, U. 1982. Electric field mediated fusion and related electric phenomena. *Biochim. Biophys. Acta.* 694:227–277.